The Journal of Chemical Physics ARTICLE scitation.org/journal/jcp

Toward the laser control of electronic decoherence

Cite as: J. Chem. Phys. 152, 184305 (2020); doi: 10.1063/5.0002166
Submitted: 22 January 2020 • Accepted: 13 April 2020 •
Published Online: 12 May 2020

Wenxiang Hu,[1] Bing Gu,[2,a)] and Ignacio Franco[2,3,b)]

AFFILIATIONS

[1] Materials Science Program, University of Rochester, Rochester, New York 14627, USA
[2] Department of Chemistry, University of Rochester, Rochester, New York 14627, USA
[3] Department of Physics, University of Rochester, Rochester, New York 14627, USA

[a)] **Current address:** Department of Chemistry, University of California Irvine, Irvine, California 92697, USA.
[b)] **Author to whom correspondence should be addressed:** ignacio.franco@rochester.edu.
URL: http://sas.rochester.edu/chm/groups/franco/

ABSTRACT

Controlling electronic decoherence in molecules is an outstanding challenge in chemistry. Recent advances in the theory of electronic decoherence [B. Gu and I. Franco, J. Phys. Chem. Lett. **9**, 773 (2018)] have demonstrated that it is possible to manipulate the rate of electronic coherence loss via control of the relative phase in the initial electronic superposition state. This control emerges when there are both relaxation and pure-dephasing channels for decoherence and applies to initially separable electron–nuclear states. In this paper, we demonstrate that (1) such an initial superposition state and the subsequent quantum control of electronic decoherence can be created via weak-field one-photon photoexcitation with few-cycle laser pulses of definite carrier envelope phase (CEP), provided the system is initially prepared in a separable electron–nuclear state. However, we also demonstrate that (2) when stationary molecular states (which are generally not separable) are considered, such one-photon laser control disappears. Remarkably, this happens even in situations in which the initially factorizable state is an excellent approximation to the stationary state with fidelity above 98.5%. The laser control that emerges for initially separable states is shown to arise because these states are superpositions of molecular eigenstates that open up CEP-controllable interference routes at the one-photon limit. Using these insights, we demonstrate that (3) the laser control of electronic decoherence from stationary states can be recovered by using a two-pulse control scheme, with the first pulse creating a vibronic superposition state and the second one inducing interference. This contribution advances a viable scheme for the laser control of electronic decoherence and exposes a surprising artifact that is introduced by widely used initially factorizable system-bath states in the field of open quantum systems.

I. INTRODUCTION

One of the greatest challenges in using molecules for quantum technologies including quantum control and quantum information is to overcome the deleterious effects due to decoherence.[1–3] Such decoherence arises from the unavoidable interactions of the system of interest with environmental degrees of freedom and limits the ability of quantum systems to fully exhibit their quantum mechanical features.[1,2,4,5] Developing methods to preserve coherence of electronic, vibrational, and vibronic degrees of freedom is essential to observe non-trivial quantum mechanical effects in molecules, to enhance molecular function through coherence,[5–13] and to exert quantum control of chemical processes[2,14] as desirable for femto- and attochemistry,[15–17] quantum information sciences,[1] and the development of enhanced spectroscopies.[18]

During decoherence, a system changes from a pure state with density matrix $\sigma(t) = |\psi\rangle\langle\psi|$ to a statistical mixture of states $\sigma(t) = \sum_i p_i|\psi_i\rangle\langle\psi_i|$ $(p_i > 0)$ due to the entanglement of the system (the degrees of freedom of interest) with the surrounding bath.[4,19] To quantify the degree of decoherence, it is useful to follow the purity defined as $\mathcal{P}(t) = \mathrm{Tr}_S[\sigma^2(t)] \leq 1$, where the trace $\mathrm{Tr}_S[O]$ is over the system degrees of freedom. Purity is a well-defined basis-independent measure of decoherence[20] that quantifies the degree of non-idempotency of the reduced density matrix of the system of

interest. The quantity $\mathcal{P} = 1$ for pure states and $\mathcal{P} < 1$ for mixed states.

A challenging and important problem in decoherence is to identify viable methods to preserve electronic coherence in molecules. Such decoherence arises due to electron–nuclear entanglement[21] and has a typical timescale of ~10 s. It accompanies photoexcitation, passage through conical intersections, electron transfer, or any other process that creates superpositions of electronic states. Its consequences can be monitored through purely electronic observables such as currents as in Refs. 22–25 or in laser spectroscopies that measure polarization response after photoexcitation. This is because the photoinduced polarization decays with the decay of electronic coherences. In fact, for a general electron–nuclear state $|\Psi(t)\rangle = \sum_i |\chi_i(t)\rangle|\phi_i\rangle$, where $\{|\phi_i\rangle\}$ are orthonormal electronic energy eigenstates and $|\chi_i(t)\rangle$ are nuclear wavepackets associated with the ith electronic state, the time-dependent dipole that determines the polarization is $\langle\mu(t)\rangle = \langle \mu_e + \mu_n\rangle = \sum_{i,j}\langle\phi_i|\mu_e|\phi_j\rangle\langle\chi_i(t)|\chi_j(t)\rangle + \sum_i\langle\chi_i(t)|\mu_n|\chi_i(t)\rangle$, where μ_e is the electronic component of the dipole operator and μ_n is the nuclear one. Thus, a decay in nuclear wave packet overlaps $|\langle\chi_j(t)|\chi_i(t)\rangle|$ for $i \neq j$ leads to a decay in the coherences of the electronic density matrix $\sigma = \sum_{i,j}\langle\chi_j(t)|\chi_i(t)\rangle|\phi_i\rangle\langle\phi_j|$, polarization $\propto\langle\mu(t)\rangle$, and electronic purity $\mathcal{P}(t) = \sum_{i,j}|\langle\chi_j(t)|\chi_i(t)\rangle|^2$.

In this context, a recently developed theory of electronic decoherence[26,27] revealed an opportunity to enhance electronic coherence through the manipulation of initial phases in an electronic superposition state. Specifically, in Refs. 26 and 27, it was demonstrated that for molecular systems with configuration-varying diabatic couplings, such as those that lead to conical intersections in the Franck–Condon region that is accessed via vertical photoexcitation, it is possible to manipulate the rate of electronic decoherence by controlling the relative phase in the initial electronic superposition state. This possibility of controlling decoherence was subsequently numerically demonstrated by Arnold *et al.*[28] They found that the control of electronic decoherence is possible, given that a coherent electronic wave packet embodying the phase difference passes through a conical intersection.

The initial theory[26,27] and subsequent simulations[28] suppose a separable initial electron–nuclear state of the form

$$|\Psi\rangle = (c_g|g\rangle + c_e|e\rangle) \otimes |\chi_0\rangle, \tag{1}$$

where $\chi_0(\mathbf{R}) = \langle\mathbf{R}|\chi_0\rangle$ is the nuclear state and $|g\rangle$ and $|e\rangle$ refer to the ground and excited electronic states, respectively. By manipulating the relative phase θ, $c_g c_e^* = |c_g\|c_e|e^{i\theta}$, of this initial superposition, it is possible to control the decoherence rate when pure-dephasing and relaxation decoherence mechanisms, the latter being opened by the diabatic couplings, are simultaneously at play. The challenge then is to physically create such a separable state with various relative phases before electronic decoherence takes place.

In this paper, we investigate the possibility of using few-cycle laser pulses to create such states and control electronic decoherence in molecules. Recent developments in ultrafast laser science allow for the production of laser pulses with just a few cycles and a well-defined carrier envelope phase φ_{CEP}.[23,24,29] The advantage of using few-cycle laser sources is that they can be used to impulsively excite the molecule in an ultrafast timescale such that the nuclear environment remains frozen during photoexcitation, as is needed to create a state of the form in Eq. (1).

Specifically, we first demonstrate that photoexcitation of a molecular system initially prepared in a separable electron–nuclear state $|\Psi(0)\rangle = |g\rangle \otimes |\chi_0\rangle$ using a few-cycle laser pulse in the weak-field limit leads to states as in Eq. (1) and to a decoherence dynamics that can be manipulated by varying the φ_{CEP}. Thus, such laser pulses, in principle, offer a possible route to exert the laser control of electronic decoherence.

Despite this progress, a key assumption in Refs. 26–28 and in the above analysis is that the molecule can be prepared in an initially separable electron–nuclear state. Such separable states are often-invoked in the theory of open quantum systems[1,4] as they are convenient in theoretical considerations. However, they are clearly an idealization. In fact, for molecules separable, electron–nuclear states only arise in the limit in which the Born–Oppenheimer approximation is exact.[21] Nevertheless, such states can be a very good approximation to the true eigenstates, e.g., for an electronic ground state that is electronically decoupled to higher lying electronic states.

Below, we examine the influence of the initial state on the laser control and show that, surprisingly, the one-photon laser control disappears when the molecule is initially prepared in a stationary molecular state. Remarkably, this happens even in situations in which the separable state is an excellent approximation to the true molecular eigenstate with fidelities above 98.5%. This is also surprising from a coherent control perspective as subsystem purity is beyond the scope of existing theorems that preclude the existence of one-photon phase control.[30,31] Thus, the often-invoked initially factorizable state introduces spurious routes for the laser control.

Through a detailed analysis of the origins of these intriguing observations, we demonstrate that the non-stationary character of the initial separable state opens interference channels that can be controlled through laser phases at the one-photon limit. We then use these insights to develop a two-pulse laser control scheme of electronic decoherence that can be used for arbitrary initial states. In it, the first pulse creates a superposition state between the desired levels, and the second pulse introduces the interference that can be used for control.

The structure of this paper is as follows: In Sec. II, we briefly summarize the theory of electronic decoherence timescales that revealed the possibility of controlling decoherence via manipulation of initial phases. Then, in Sec. III, we introduce our computational methods and the exemplifying (photoisomerization and displaced harmonic oscillator) models employed to test the feasibility of implementing such a theory through actual laser photoexcitation. The achieved laser control of electronic decoherence from initially separable states in these models and its disappearance from stationary states are discussed in Secs. IV A and IV B. Then, in Sec. IV C, we provide an analysis of these phenomena in the context of a minimal analytical model that captures the essential features of the problem. In Sec. IV D, we summarize our main findings and discuss the qualitative origin and the minimum requirements for the laser phase control of electronic decoherence. Based on this analysis, in Sec. V, we propose a laser control strategy of

electronic decoherence that can be employed for arbitrary initial states.

II. THEORY OF ELECTRONIC DECOHERENCE TIMESCALES

In the interest of clarity, we first summarize the theory of electronic decoherence timescales that forms the starting point of this analysis. Consider a system interacting with an environment with Hamiltonian $H = H_S + H_B + H_{SB}$, where H_S describes the system, H_B describes the bath, and

$$H_{SB} = \sum_\alpha S_\alpha \otimes B_\alpha \tag{2}$$

describes their interaction. Here, S_α refers to an operator in the Hilbert space of the system, while B_α are operators in the Hilbert space of the bath. To define a decoherence time, in Ref. 26, we assumed that the system is initially in a pure state that decoheres as a result of the dynamics. This implies that at initial time, the system–bath state $\rho(0) = \sigma(0) \otimes \rho_B(0)$ is not entangled and the purity $\mathcal{P}(0) = 1$, where $\rho_B(t)$ is the reduced density matrix for the bath. To capture the early time purity dynamics, we performed a second order expansion of the Liouville–von Neumann equation satisfied by the composite system $i\hbar\frac{d}{dt}\rho = [H, \rho]$ around initial time $t = 0$, $\rho(t) = \rho(0) + t\,\frac{d}{dt}\rho(t)\big|_{t=0} + \frac{t^2}{2}\,\frac{d^2}{dt^2}\rho(t)\Big|_{t=0}$. By tracing over the bath to obtain a short-time expansion of the density matrix of the system $\sigma(t)$ and calculating purity, we isolated a general and simple relation for the initial purity decay. The procedure revealed that for early times, the purity decays like a Gaussian $\mathcal{P}(t) = e^{-t^2/\tau_d^2}$ with the decoherence timescale

$$\tau_d = \hbar\left(2\sum_{\alpha\beta}\Delta^B_{\alpha\beta}\times\Delta^S_{\alpha\beta}\right)^{-1/2}. \tag{3}$$

Here, $\Delta^S_{\alpha\beta} \equiv \langle S_\alpha S_\beta\rangle - \langle S_\alpha\rangle\langle S_\beta\rangle$ and $\Delta^B_{\alpha\beta} = \langle B_\alpha B_\beta\rangle - \langle B_\alpha\rangle\langle B_\beta\rangle$ are the initial-time crossed fluctuations (covariances) of the system and the bath operators entering H_{SB}. If the long time limit of the system purity $\mathcal{P}_\infty \equiv \lim_{t\to\infty}\mathcal{P}(t)$ is known, one can interpolate the short and asymptotic purity behavior as $\mathcal{P}(t) - \mathcal{P}_\infty \approx (1-\mathcal{P}_\infty)e^{-(1-\mathcal{P}_\infty)^{-1}(t/\tau_d)^2}$.

The result in Eq. (3) is universal. It applies to any initially pure system in interaction with a bath and does not invoke common approximations employed in open quantum system dynamics, such as Markovian dynamics, harmonic baths, or rotating-wave approximations. The physical idea conveyed by Eq. (3) is that the larger the quantum fluctuations of the operators that enter into H_{SB} at initial time the faster the decoherence. The Gaussian shape of the decoherence decay is fundamental and can be regarded as a consequence of the quantum Zeno effect.[32] The often-assumed exponential coherence decay arises in the particular limit in which the environment is Markovian.[4] Such a limit is beyond the applicability of the early time expansion.

Equation (3) makes it straightforward to calculate decoherence timescales for any system–bath model. In particular, in Ref. 27, we used it to develop a generalized theory of electronic decoherence in molecules that we now summarize. Consider a general two-surface molecular Hamiltonian of the form

$$\begin{aligned} H_M &= H_g|g\rangle\langle g| + H_e|e\rangle\langle e| + V_{ge}(\mathbf{R})|g\rangle\langle e| + V_{eg}(\mathbf{R})|e\rangle\langle g| \\ &= H_g\otimes\mathcal{I}_e + \mathcal{E}_{eg}(\mathbf{R})|e\rangle\langle e| + V_{ge}(\mathbf{R})|g\rangle\langle e| + V_{eg}(\mathbf{R})|e\rangle\langle g|. \end{aligned} \tag{4}$$

Here, $|g\rangle$ and $|e\rangle$ refer to electronic ground and excited diabatic states (eigenstates of the electronic Hamiltonian of the molecule for a fixed reference nuclear geometry $\mathbf{R}_0$), respectively. The operators $H_g = T_N + V_g(\mathbf{R})$ and $H_e = T_N + V_e(\mathbf{R})$ denote the nuclear Hamiltonians in ground and excited electronic states, respectively, $\mathcal{I}_e$ is the identity in electronic subspace, and $\mathcal{E}_{eg}(\mathbf{R}) \equiv H_e - H_g$ is the energy gap operator between the ground and excited diabatic potential energy surfaces (DPES). The quantity $V_{ge}(\mathbf{R})$ $\left[= V^*_{eg}(\mathbf{R})\right]$ represents the diabatic couplings between DPES caused by the electron–nuclear couplings.

To apply the theory of decoherence timescales, the molecule is taken to be in a initially separable electron–nuclear state $\rho(0) = \sigma(0)\otimes\rho_B(0)$, where the electronic state $\sigma(0) = |\psi\rangle\langle\psi|$ is a superposition $|\psi\rangle = (c_g|g\rangle + c_e|e\rangle)$. The electron–nuclear interaction terms in Eq. (4) are of the form in Eq. (2) and thus can be directly inserted into Eq. (3) to generate a timescale for electronic decoherence,

$$\begin{aligned} \tau_d^{-2} = \frac{2}{\hbar^2}\Big[&|c_g|^2|c_e|^2\langle\delta^2\mathcal{E}_{eg}\rangle + (1-4|c_g|^2|c_e|^2\cos^2\theta)\langle\delta^2 V_{eg}\rangle \\ &+ 2(|c_g|^2-|c_e|^2)|c_g\|c_e|\cos\theta\langle\delta\mathcal{E}_{eg}\delta V_{eg}\rangle\Big]. \end{aligned} \tag{5}$$

Here, θ is the relative phase in the initial superposition $c_g c_e^\star = |c_g\|c_e|e^{i\theta}$, $\delta O = O - \langle O\rangle$, and $\delta^2 O = O^2 - \langle O\rangle^2$, where $\langle O\rangle \equiv \mathrm{Tr}\{\rho(0)O\} = \mathrm{Tr}_B\{\rho_B(0)O\}$ for O defined in the nuclear Hilbert space.

The physical meaning of the terms in τ_d is as follows: The first term due to the quantum fluctuations of the energy gap ($\langle\delta^2\mathcal{E}_{eg}\rangle$) is the decoherence between two DPES that represent pure-dephasing effects previously identified by Rossky.[33] It is pure-dephasing because it leads to decoherence without net exchange of energy between the system and surroundings as it arises from the $\mathcal{E}_{eg}(\mathbf{R})|e\rangle\langle e|$ term in the Hamiltonian. In addition, the theory reveals that electronic transitions among diabatic states induced by the nuclei introduce an additional important channel for electronic decoherence quantified by the term proportional to $\langle\delta^2 V_{eg}\rangle$. Such electronic transitions and the resulting energy exchange between electrons and nuclei are necessary for the emergence of relaxation. Surprisingly, contrary to Bloch equations ideas where dephasing and relaxation effects contribute separately to decoherence,[34] we find that these two contributions interfere as revealed by the third term in Eq. (5). For definitiveness, Eq. (5) focuses on two-surface models. However, the theory has been extended to the many-surface case.[27]

Importantly, the theory reveals that when both relaxation and pure dephasing effects are at play, it is possible to control the decoherence rate by simply changing the phase θ of the initial superposition, thus opening opportunities for the quantum control of decoherence. Such θ dependent terms arise when the diabatic couplings $V_{ge}(\mathbf{R})$ vary spatially with $\mathbf{R}$ such that their initial-state fluctuations are non-zero. This is the case, for example, in conical

intersections and underlies the observations in Ref. 28. However, conical intersections are not a necessary requirement.

The phase dependence in the purity can be employed to enhance or suppress the decoherence with respect to what would have been obtained if such phase was uncontrollable. To see this, contrast the purity dynamics for a given θ, $\mathcal{P}(\theta)$, with that obtained by considering θ as a uniformly distributed random variable, $\mathcal{P}_{\rm in} = \frac{1}{2\pi}\int_0^{2\pi} d\theta \mathcal{P}(\theta)$. Their difference

$$\mathcal{P}(t) - \mathcal{P}_{\rm in}(t) = \frac{4t^2}{\hbar^2}\left[|c_g|^2|c_e|^2\cos(2\theta)\langle\delta^2 V_{eg}\rangle - (|c_g|^2 - |c_e|^2) \times |c_g||c_e|\cos\theta\langle\delta\mathcal{E}_{eg}\delta V_{eg}\rangle\right] + \mathcal{O}(t^4) \quad (6)$$

can be positive or negative, indicating that the phase dependence can be used to mitigate or enhance the decoherence.

III. MODEL AND METHODS

To study the possibility of using lasers to control electronic decoherence, we simulated the decoherence dynamics in a model of internal torsion photoisomerization (Model I) and a displaced harmonic oscillator model (Model II), which are two basic models for the photoexcited dynamics of molecules. We focus on minimal exemplifying models with two electronic states and one nuclear degree of freedom. As shown in Ref. 35, one nuclear degree of freedom is enough to induce the electronic coherence loss. The models are generic enough to reveal the basic features of the laser control.

A. Model I: Photoisomerization

Model I describes photoisomerization along a torsional coordinate ϕ with DPES shown in Fig. 1(a). It is adapted from the model in Ref. 36 for the *cis–trans* photoisomerization of rhodopsin. Here, in the notation of Eq. (4), $H_g = -\frac{1}{2I}\frac{d^2}{d\phi^2} + \frac{1}{2}W_g(1-\cos\phi)$ and $H_e = -\frac{1}{2I}\frac{d^2}{d\phi^2} + \hbar\omega_0 - \frac{1}{2}W_e(1-\cos\phi)$, where $\hbar\omega_0$ denotes the vertical transition energy of $\phi = 0, \pi$, I is the moment of inertia, and W_n $(n = g, e)$ denotes the first coefficient of the Fourier series expansion of the periodic torsional potential. As diabatic couplings, we choose $V_{ge} = V_{eg} = \lambda_0 - \lambda_1\cos\phi$, where λ_0 and λ_1 characterize the strength of the constant and space-dependent diabatic couplings, respectively. This type of coupling respects the periodic nature of the DPES. Furthermore, for $\lambda_1 \neq 0$, the fluctuations $\langle\delta^2 V_{eg}\rangle$ and $\langle\delta\mathcal{E}_{eg}\delta V_{eg}\rangle$ in Eq. (5) are non-zero, and coherent control of electronic decoherence should, in principle, be possible (Sec. II).

Contrary to the rhodopsin model in Ref. 36, for simplicity, this model only has one nuclear degree of freedom, and the diabatic coupling is taken to be along the torsional coordinate. In the simulations, we employ the same parameters identified for the rhodopsin model with $\hbar\omega_0 = 2.48$ eV, $I^{-1} = 4.84\times10^{-4}$ eV, $W_g = 3.6$ eV, and $W_e = 1.09$ eV. The laser control of electronic decoherence for molecular systems with space-dependent ($\lambda_0 = 0$ eV and $\lambda_1 = 0.19$ eV), constant ($\lambda_0 = 0.19$ eV and $\lambda_1 = 0$ eV), and zero ($\lambda_0 = \lambda_1 = 0$ eV) diabatic couplings are studied in Sec. IV.

B. Model II: Displaced harmonic oscillator

Model II is a one-dimensional displaced harmonic oscillator model with DPES shown in Fig. 1(b). In this model, $H_g = -\frac{\hbar^2}{2m}\frac{d^2}{dx^2} + \frac{1}{2}K_g(x-x_g)^2$ and $H_e = -\frac{\hbar^2}{2m}\frac{d^2}{dx^2} + \hbar\omega_0 + \frac{1}{2}K_e(x-x_e)^2$, where x is a dimensionless nuclear coordinate.[37,38] Here, m is the nuclear effective mass, K_n $(n = g, e)$ is the force constant, and x_n $(n = g, e)$ indicates the equilibrium nuclear geometry of the nth diabatic potential energy surface. As diabatic couplings, we choose $V_{ge} = V_{eg} = \lambda_0 + \lambda_1 x$, where λ_0 and λ_1 characterize the strength of the constant and the space dependent diabatic couplings, respectively. For $\lambda_1 \neq 0$, the fluctuations $\langle\delta^2 V_{eg}\rangle$ and $\langle\delta\mathcal{E}_{eg}\delta V_{eg}\rangle$ in Eq. (5) are non-zero as required by the theory for the emergence of quantum control of electronic decoherence. In this model, the values of parameters are chosen as $m = 86.65$ eV fs^2, $\hbar\omega_0 = 0.44$ eV, $K_{g,e} = 0.02$ eV, $x_g = -8.67$, and $x_e = 5.62$. The molecular systems with the space dependent ($\lambda_0 = 0$ eV and $\lambda_1 = 0.02$ eV), constant ($\lambda_0 = 0.19$ eV and $\lambda_1 = 0$ eV), and zero ($\lambda_0 = \lambda_1 = 0$ eV) diabatic couplings are studied in Sec. IV. As described below, for these parameters, the decoherence process can be slower than the photoexcitation process as required to generate states of the form in Eq. (1).

C. Laser induced dynamics

To photoexcite the model molecules, we employ a 2 fs few-cycle Gaussian laser pulse. Such a short laser pulse enables impulsive excitation and generating states of the form in Eq. (1). Through such excitation, we assess the possibility of enacting the theory of electronic decoherence through actual laser photoexcitation. The vector potential $\vec{A}(t)$ associated with the electric field $\vec{F}(t) = -\dot{\vec{A}}(t)$ of such

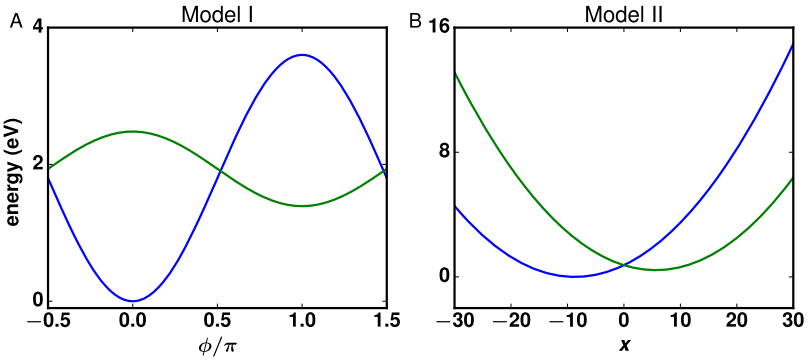

FIG. 1. The diabatic potential energy surfaces of (a) Model I describing photoisomerization along a torsional coordinate ϕ and (b) Model II describing a displaced harmonic oscillator model. The blue (green) lines refer to the ground (excited) electronic diabatic state.

laser can be described as

$$\vec{A}(t) = \vec{\epsilon}(F_0/\omega)\exp[-(t-t_c)^2/t_w^2]\sin(\omega(t-t_c)+\varphi_{CEP}). \quad (7)$$

Here, $\vec{\epsilon}$ is the unit polarization vector, $t_w = 2$ fs is the pulse width, F_0 is the pulse amplitude at pulse center $t_c = 7$ fs, ω is the central frequency, and φ_{CEP} is the carrier envelope phase (CEP). This form guarantees that the electric field $\vec{F}(t) = \vec{\epsilon}F(t)$ is an ac source as $\int_{-\infty}^{\infty}\vec{F}(t)dt = \vec{A}(-\infty) - \vec{A}(\infty) = 0$. In this case,

$$F(t) = -F_0 e^{-\frac{(t-t_c)^2}{t_w^2}}\cos(\omega(t-t_c)+\varphi_{CEP}) + \frac{F_0}{\omega}e^{-\frac{(t-t_c)^2}{t_w^2}}\sin(\omega(t-t_c)+\varphi_{CEP})\frac{2(t-t_c)}{t_w^2}, \quad (8)$$

where the second term in the expression of $F(t)$ guarantees that the pulse remains as an ac source even in the few-cycle limit.

The light–matter interaction H_{RM} is described in dipole approximation where $H_{RM} = -\vec{\mu}\cdot\vec{F}(t)$. Assuming that the neutral molecular system does not have a permanent dipole moment, $H_{RM} = -F(t)\,(\mu_{ge}|g\rangle\langle e| + \mu_{eg}|e\rangle\langle g|)$ with $\mu_{ge} = \mu_{eg} = \langle g|\vec{\mu}\cdot\vec{\epsilon}|e\rangle$ and $\mu_{gg} = \mu_{ee} = 0$. The total time-dependent Hamiltonian $H_T(t) = H_M + H_{RM}(t)$ is

$$H_T(t) = H_g|g\rangle\langle g| + H_e|e\rangle\langle e| + (V_{ge}(\mathbf{R}) - \mu_{ge}F(t))|g\rangle\langle e| + (V_{eg}(\mathbf{R}) - \mu_{eg}F(t))|e\rangle\langle g|. \quad (9)$$

The central laser frequency $\hbar\omega = (V_e(\mathbf{R}_g) - V_g(\mathbf{R}_g)) = 2.48$ eV is chosen to be at resonance with the energy difference between the two surfaces at the ground-state nuclear equilibrium geometry $\mathbf{R}_g$ in both cases. Here, $\mathbf{R}$ refers to the ϕ coordinate for Model I and the x coordinate for Model II. Furthermore, throughout, we choose a laser amplitude such that $|F_0\mu_{ge}| = 0.09$ eV. This guarantees that the laser is in the weak-field limit, where the magnitude of the excited state amplitude $|c_e|$ increases linearly with the laser amplitude $|F_0|$ (see Fig. S1 of the supplementary material).

The quantum dynamics is propagated using a multi-state split operator method in the Condon approximation.[39] We employ a time step propagation $\Delta t_1 = 0.0005$ fs during the laser excitation and $\Delta t_2 = 0.001$ fs after the laser pulse. For Model I, periodic boundary conditions are used with a period range of $[-\pi/2, 3\pi/2]$ and $N = 1024$ grids points. For Model II, the grid is defined in the $[-24.38, 35.62]$ range with $N = 1024$ grid points. Results were checked for convergence by checking for energy conservation after the laser pulse (Fig. S2), and invariance of the results by decreasing the time step (Fig. S3) and the number of grid points N (Fig. S4).

IV. LASER CONTROL WITH A FEW-CYCLE LASER PULSE

A. Laser control starting from initially separable states

We first focus on the laser control of electronic decoherence when the system is initially prepared in a separable electron–nuclear state of the form

$$|\Psi_{sp}(0)\rangle = |g\rangle\otimes|\chi_0\rangle. \quad (10)$$

While clearly an idealization, initially separable system–bath states are often assumed when dealing with open quantum systems as they simplify theoretical considerations and can be an accurate representation to the true eigenstates. In particular, they are the starting point of previous analyses that showed that electronic decoherence can be controlled by manipulating the relative phase of the model superposition in Eq. (1).[26–28] Here, we study the possibility of generating the state in Eq. (1) through actual laser photoexcitation from Eq. (10) as needed for the physical realization of this possible route for the coherent control of electronic decoherence.

The initial vibrational state is taken to be the ground state of the ground diabatic surface for both models. In particular, for Model I, it is given by

$$\chi_g(\phi) = \langle\phi|\chi_g\rangle = \left(\sqrt{\frac{W_g I}{2}}\frac{1}{\pi}\right)^{\frac{1}{4}} e^{-\sqrt{\frac{W_g I}{2}}\frac{\phi^2}{2}}. \quad (11)$$

This state is obtained by performing a harmonic approximation of the ground torsional potential around $\phi = 0$. Similarly, for Model II, the initial state is

$$\chi_g(x) = \langle x|\chi_g\rangle = \left(\frac{1}{\pi}\right)^{\frac{1}{4}} e^{-(x-x_g)^2/2}. \quad (12)$$

In the photoexcitation, we employ a few-cycle laser pulse of width $t_w = 2$ fs of the form in Eq. (8). Such a short laser pulse is expected to create an exact replica of the vibrational wavepacket in the excited state potential energy surface leading to a state as that in Eq. (1).

1. Intersection model ($\lambda_0 = 0$ and $\lambda_1 \neq 0$)

We first focus on the laser-induced dynamics when $\lambda_0 = 0$ and $\lambda_1 \neq 0$. In this case, both Model I and Model II have space-varying diabatic couplings as needed for the emergence of relative-phase control of electronic decoherence in Eq. (5). These models develop conical intersections in higher dimensional configurational space.[38] Figures 2 and 3 show the decoherence dynamics during and after photoexcitation for Model I and Model II, respectively. At initial times, the curves coincide as all cases start from a pure state. However, the *early time* dynamics where the decoherence decays like a Gaussian strongly depends on the CEP. As shown, changing the CEP of the laser pulse leads to significantly different rates of electronic coherence loss and can be used to suppress or enhance the decoherence rate. Note that the net energy absorbed by the system during photoexcitation also depends on the CEP (see Fig. S2). However, once the diabatic couplings are turned off and the dynamics becomes pure dephasing ($\lambda_0 = \lambda_1 = 0$), all decoherence dynamics coincide and the phase control is lost. This behavior is consistent with Eq. (5) that indicates that for pure dephasing dynamics, only the first term due to the quantum fluctuations of the energy gap ($\langle\delta^2\mathcal{E}_{eg}\rangle$) determines the electronic decoherence between two DPES, and such a term does not depend on the relative phase.

Thus, the laser control of electronic decoherence can be achieved in both models when the dynamics starts from a separable state and the diabatic couplings are non-zero and space-dependent. This observation is what would have been expected from the theory of electronic decoherence timescales summarized in Sec. II.

We note that due to the low dimensionality of the models employed, here and throughout, partial revivals of purity are observed at longer times (see Fig. S5). Such partial revivals have

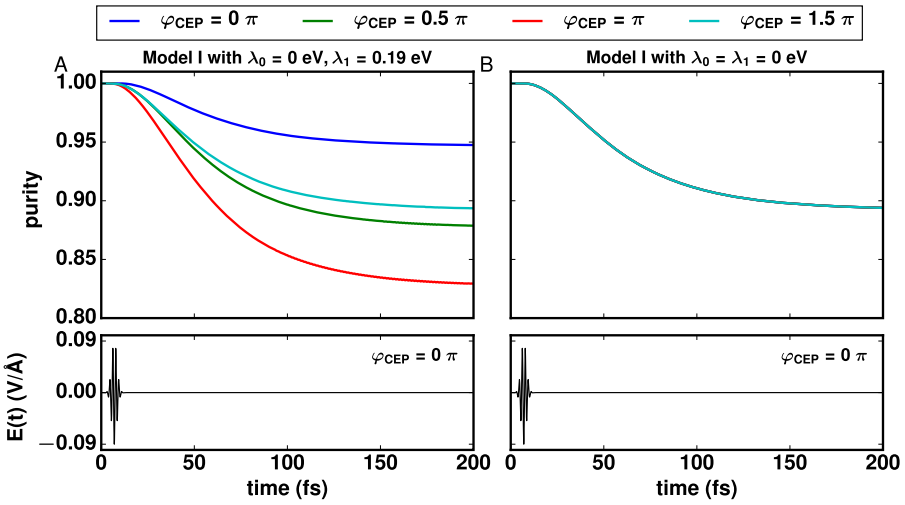

FIG. 2. [(a) and (b)] Laser control of electronic decoherence in Model I starting from a separable electron–nuclear state. The plot shows the purity dynamics during and after photoexcitation with a few-cycle laser pulse with various CEPs. The top panels contrast the purity dynamics with non-zero (λ_1 = 0.19 eV) and zero (λ_1 = 0 eV) space dependent diabatic couplings, while λ_0 = 0. The bottom panels show the employed 2 fs laser pulse for φ_{CEP} = 0.

been described in details elsewhere[35] and are not expected in higher dimensional systems where the electronic decoherence dynamics is dominated by the initial Gaussian purity decay.[40,41]

2. Avoided crossing model ($\lambda_0 \neq 0$ and $\lambda_1 = 0$)

The theoretical analysis in Sec. II indicates that the laser control of electronic decoherence requires space-dependent diabatic couplings for which $\delta V_{eg} \neq 0$ (or $\lambda_1 \neq 0$ in this case). To determine if the control survives even when $\lambda_1 = 0$ (but $\lambda_0 \neq 0$), we computed the decoherence dynamics with $\lambda_1 = 0$ in both models. In this case (Fig. 4), changing the CEP leads to significantly different rates of electronic coherence loss for both Model I and Model II that go beyond the theory in Sec. II. Here, to make these models comparable, the constant diabatic coupling strength is set as λ_0 = 0.19 eV for both models.

To demonstrate that this feature is inherent to the system and not to the photoexcitation process, we propagated the dynamics of both models starting with an initial superposition $|\Psi\rangle = (\sqrt{\frac{2}{3}}e^{i\theta}|g\rangle + \sqrt{\frac{1}{3}}|e\rangle) \otimes |\chi_0\rangle$. The results, shown in Fig. S6, show clear modulation of the purity dynamics by changing θ, which demonstrates that this is an effect that goes beyond the early time expansion in Refs. 26 and 27.

B. Laser control starting from eigenstates

The results above indicate that it is possible to use few-cycle laser pulses to create states of the form in Eq. (1) and control the electronic decoherence by varying the CEP. Despite these encouraging results, one important assumption thus far has been the use of a factorizable initial electron–nuclear state Eq. (10). The impulsive excitation of such a state retains the initially factorizable form to generate a state like that in Eq. (1) used in previous theory and simulations.[27,28] We now investigate how the laser control is modified when the system is initially prepared in a stationary state of

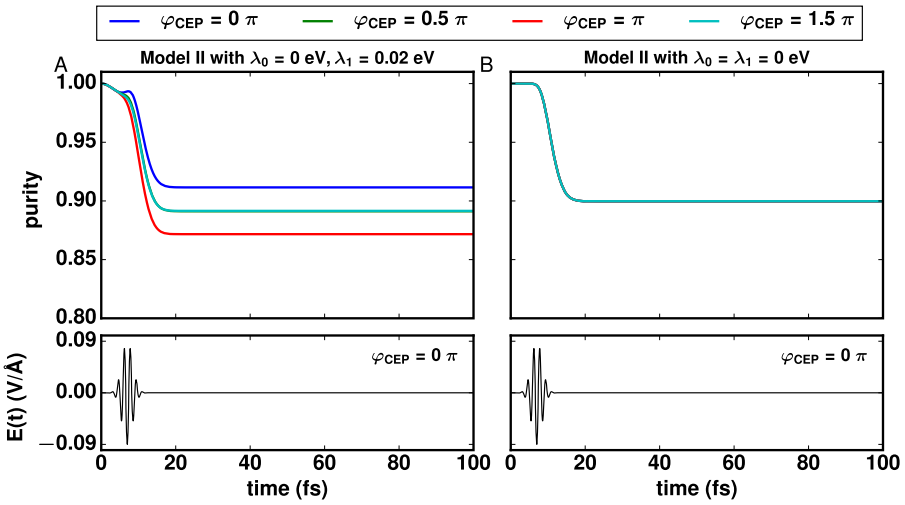

FIG. 3. [(a) and (b)] Laser control of electronic decoherence in Model II starting from a separable electron–nuclear state. The organization of the plot is identical to that in Fig. 2.

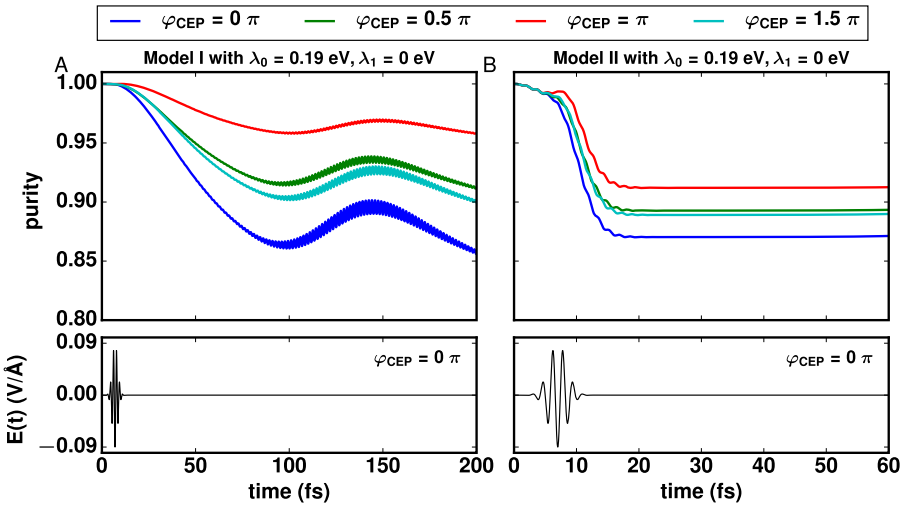

FIG. 4. [(a) and (b)] Laser control of electronic decoherence starting from a separable electron–nuclear state for models with space-independent diabatic couplings ($\lambda_0 \neq 0$, $\lambda_1 = 0$). The plot shows the purity dynamics during and after photoexcitation with a few-cycle laser pulse with various CEPs when $\lambda_0 = 0.19$ eV and $\lambda_1 = 0$ eV. The bottom panels show the employed 2 fs laser pulse for $\varphi_{CEP} = 0$.

the molecular Hamiltonian. Such states are readily available through cooling or laser purification.

Specifically, as an initial state, we choose the ground vibronic state $|\Psi_g(0)\rangle$ obtained by directly diagonalizing the molecular Hamiltonian. In the diagonalization, the Hamiltonian in Eq. (4) is represented in the tensor product basis of diabatic electronic states and a grid representation for the nuclei by

$$\begin{aligned} H_M = \sum_{\mathbf{R},\mathbf{R}'} \big[& (\langle \mathbf{R}|T_N|\mathbf{R}'\rangle + V_g(\mathbf{R})\delta_{\mathbf{R}\mathbf{R}'})|g\rangle\langle g| \\ & + (\langle \mathbf{R}|T_N|\mathbf{R}'\rangle + V_e(\mathbf{R})\delta_{\mathbf{R}\mathbf{R}'})|e\rangle\langle e| \\ & + V_{ge}(\mathbf{R})\delta_{\mathbf{R}\mathbf{R}'}|g\rangle\langle e| + V_{eg}(\mathbf{R})\delta_{\mathbf{R}\mathbf{R}'}|e\rangle\langle g|\big]|\mathbf{R}\rangle\langle \mathbf{R}'|, \end{aligned} \tag{13}$$

with

$$\begin{aligned} \langle \mathbf{R}|T_N|\mathbf{R}'\rangle &= \sum_{\mathbf{k},\mathbf{k}'} \langle \mathbf{R}|\mathbf{k}\rangle\langle \mathbf{k}|\frac{\hbar^2\mathbf{k}^2}{2m}|\mathbf{k}'\rangle\langle \mathbf{k}'|\mathbf{R}'\rangle \\ &= \sum_{\mathbf{k}} \frac{1}{N}\exp[i\mathbf{k}\cdot(\mathbf{R}-\mathbf{R}')]\frac{\hbar^2\mathbf{k}^2}{2m}. \end{aligned} \tag{14}$$

The exact decoherence dynamics for Model I and II induced via resonant photoexcitation with a 2 fs laser is shown in Fig. 5 ($\lambda_0 = 0$ and $\lambda_1 \neq 0$) and Fig. 6 ($\lambda_0 \neq 0$ and $\lambda_1 = 0$), respectively. In striking contrast with the observations in Sec. IV A, changing the CEP of the laser pulse has no significant influence on the purity dynamics in all cases. This is particularly surprising when one realizes that the factorizable initial states $|\Psi_{sp}(0)\rangle$ used in Sec. IV A closely

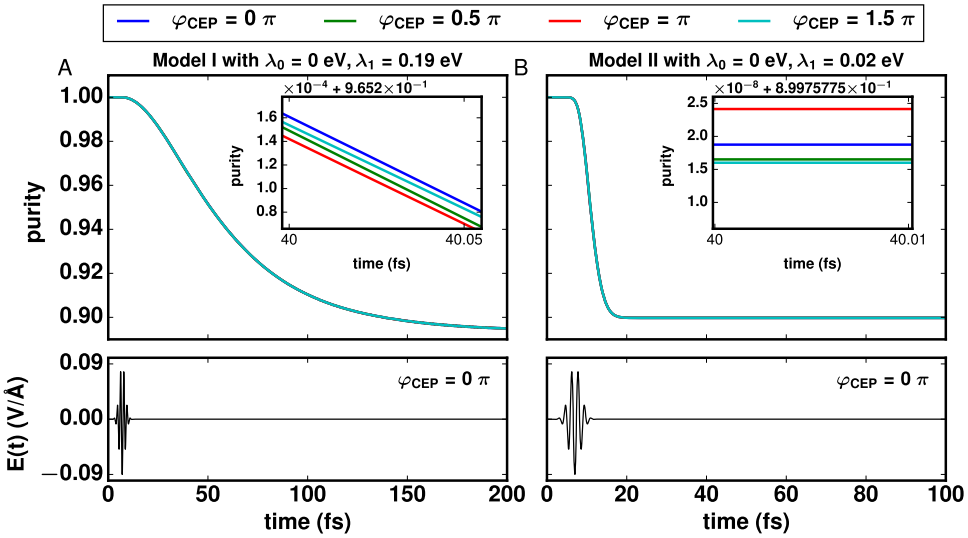

FIG. 5. [(a) and (b)] Electronic decoherence dynamics during and after photoexcitation starting from a vibronic eigenstate. The plot shows the purity dynamics during and after photoexcitation with a few-cycle laser pulse for various CEPs. The bottom panel shows the 2 fs laser pulse employed for photoexcitation with phase $\varphi_{CEP} = 0$. Note that there is no appreciable laser phase control even for $\lambda_1 \neq 0$ as all curves essentially overlap. A magnification of the plots (inset) reveals that the control is negligible but nonzero.

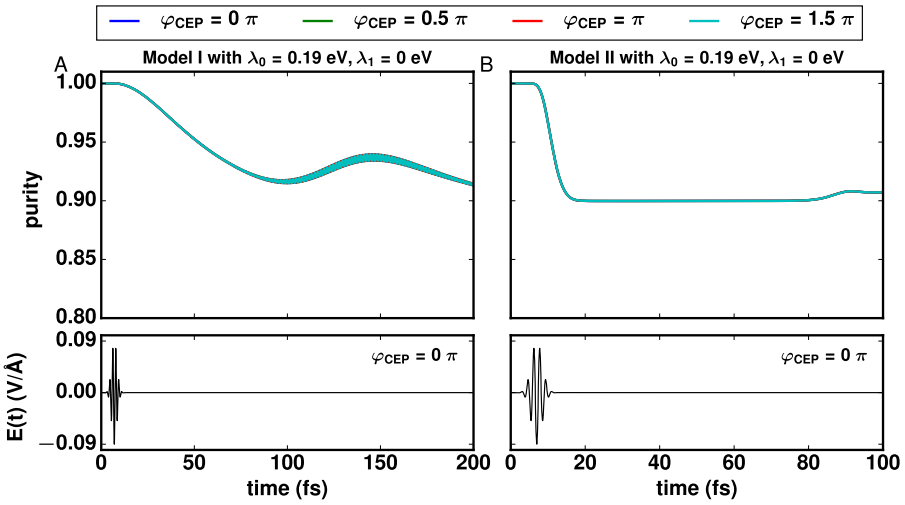

FIG. 6. [(a) and (b)] Electronic decoherence dynamics during and after photoexcitation starting from a vibronic eigenstate for space independent diabatic couplings ($\lambda_0 \neq 0$, $\lambda_1 = 0$). The plot shows the purity dynamics during and after photoexcitation with a few-cycle laser pulse for various CEPs. Note that there is no appreciable CEP control. The bottom panel shows the 2 fs laser pulse employed for photoexcitation with phase $\varphi_{CEP} = 0$.

resemble the stationary states $|\Psi_g(0)\rangle$ used in Figs. 5 and 6 with a fidelity $|\langle\Psi_{sp}(0)|\Psi_g(0)\rangle|^2$ of 0.9942 for Model I and 0.9873 for Model II. That is, even when the initial separable state is an excellent approximation to the true molecular ground state, it leads to qualitatively different behavior under laser excitation.

C. Minimal theoretical model

The simulations above demonstrate that when the dynamics is initiated from a separable electron–nuclear state, it is possible to exert laser coherent control of the decoherence. However, all laser control dies when a vibronic eigenstate is employed as the initial state even in cases where the factorizable initial state is an excellent approximation to the true eigenstate. To understand the physical principles behind these observations, we analytically study the laser control in a minimal model that captures the essential physics.

1. Hamiltonian

For simplicity, we focus on a minimal vibronic system with a Hilbert space spanned by two states $|g\rangle|\chi_g\rangle$ and $|e\rangle|\chi_e\rangle$, where $|\chi_g\rangle$ and $|\chi_e\rangle$ are purely nuclear states. In this basis, the molecular Hamiltonian in Eq. (4) is

$$H_M = \begin{pmatrix} E_g & \Lambda \\ \Lambda & E_e \end{pmatrix}, \tag{15}$$

where $E_g = \langle\chi_g|H_g|\chi_g\rangle$, $E_e = \langle\chi_e|H_e|\chi_e\rangle$, and $\Lambda = \langle\chi_g|V_{ge}|\chi_e\rangle = \langle\chi_e|V_{eg}|\chi_g\rangle$. The eigenstates of this Hamiltonian are

$$\begin{aligned} |E_0\rangle &= \cos\alpha|\varepsilon_g\rangle|\chi_g\rangle + \sin\alpha|\varepsilon_e\rangle|\chi_e\rangle, \\ |E_1\rangle &= -\sin\alpha|\varepsilon_g\rangle|\chi_g\rangle + \cos\alpha|\varepsilon_e\rangle|\chi_e\rangle, \end{aligned} \tag{16}$$

with corresponding eigenenergies $E_0 = \bar{E} - \sqrt{\Delta^2 + \Lambda^2}$ and $E_1 = \bar{E} + \sqrt{\Delta^2 + \Lambda^2}$ with $\bar{E} = (E_g + E_e)/2$ and $\Delta = (E_e - E_g)/2$. Here, the mixing angle α is defined as $\sin(2\alpha) = -\Lambda/\sqrt{\Delta^2 + \Lambda^2}$ and $\cos(2\alpha) = \Delta/\sqrt{\Delta^2 + \Lambda^2}$. Conversely, the separable states can be represented in the basis of eigenstates as

$$\begin{aligned} |\varepsilon_g\rangle|\chi_g\rangle &= \cos\alpha|E_0\rangle - \sin\alpha|E_1\rangle, \\ |\varepsilon_e\rangle|\chi_e\rangle &= \sin\alpha|E_0\rangle + \cos\alpha|E_1\rangle. \end{aligned} \tag{17}$$

The electronic purity of an arbitrary state $|\Psi(t)\rangle = a(t)|\varepsilon_g\rangle|\chi_g\rangle + b(t)|\varepsilon_e\rangle|\chi_e\rangle$ in this model is given by

$$\mathcal{P}(t) = |a(t)|^4 + |b(t)|^4 + 2|a(t)|^2|b(t)|^2|S|^2, \tag{18}$$

where $S = \langle\chi_g|\chi_e\rangle \neq 0$ is the overlap between nuclear states.

2. First order perturbation theory

We are interested in the electronic purity after photoexcitation. Since the control is in the weak-field one-photon limit, we limit our considerations to first-order perturbation theory in the laser–matter interaction. Let $H_T(t) = H_M + H_{RM}(t)$, where $H_{RM} = -\vec{\mu}\cdot\vec{F}(t)$ is the perturbation due to the laser. To the first order in perturbation theory,[42] $|\Psi(t)\rangle = |\Psi^{(0)}(t)\rangle + |\Psi^{(1)}(t)\rangle$, where $|\Psi^{(0)}(t)\rangle = e^{-\frac{i}{\hbar}H_M t}|\Psi^{(0)}(0)\rangle$ represents the perturbation-free evolution of the system and

$$|\Psi^{(1)}(t)\rangle = \frac{1}{i\hbar}\int_0^t dt' e^{-\frac{i}{\hbar}H_M(t-t')}H_{RM}(t')e^{-\frac{i}{\hbar}H_M t'}|\Psi^{(0)}(0)\rangle \tag{19}$$

is the photoexcited component. The state at $t = 0$ can be represented in the basis of eigenstates of H_M as $|\Psi^{(0)}(0)\rangle = \sum_n c_n|E_n\rangle$. In this basis,

$$\begin{aligned} |\Psi^{(1)}(t)\rangle &= \frac{i}{\hbar}\sum_{n,n'}\int_0^t dt' F(t') e^{-i\omega_{n'n}t'}\mu_{n'n}e^{-\frac{i}{\hbar}E_{n'}t}c_n|E_{n'}\rangle \\ &\approx \frac{i}{\hbar}\sum_{n,n'}\left[\int_{-\infty}^{\infty} dt' F(t') e^{i\omega_{nn'}t'}\right]\mu_{n'n}e^{-\frac{i}{\hbar}E_{n'}t}c_n|E_{n'}\rangle, \end{aligned} \tag{20}$$

where $\mu_{n'n} = \langle E_{n'}|\vec{\mu}\cdot\vec{\epsilon}|E_n\rangle$ is the transition dipole between states $|E_n\rangle$ and $|E_{n'}\rangle$ and $\omega_{nn'} = \frac{E_{n'} - E_n}{\hbar}$ is the transition frequency. For simplicity of presentation, we take $t_c = m2\pi/\omega_{nn'}$ with positive integers m

such that $t_c - 2t_w > 0$. In this case, the lower limit of the integral in the above equations can be extended to $-\infty$ as the amplitude of the electric field is negligible for $t < 0$. Similarly, the upper limit can be extended to $+\infty$ as we are only interested in $t \gg t_c + 2t_w$ when the pulse is over. Under such conditions, the time integral in Eq. (20) becomes

$$\epsilon(\omega_{nn'}) = \int_{-\infty}^{\infty} dt' F(t') e^{i\omega_{nn'}t'} = \frac{F_0\sqrt{\pi}t_w}{2\omega}\omega_{nn'} e^{-\frac{t_w^2(\omega+\omega_{nn'})^2}{4}} e^{i\varphi_{CEP}} - \frac{F_0\sqrt{\pi}t_w}{2\omega}\omega_{nn'} e^{-\frac{t_w^2(\omega-\omega_{nn'})^2}{4}} e^{-i\varphi_{CEP}}, \tag{21}$$

where we have used Eq. (8). For absorption (or stimulated emission), $\omega \approx \omega_{nn'} > 0$ (or $\omega \approx -\omega_{nn'}$) and the system picks a phase $-e^{-i\varphi_{CEP}}$ (or $-e^{i\varphi_{CEP}}$) during photoexcitation, i.e., $\epsilon(\omega_{nn'}) = -|\epsilon(\omega_{nn'})|e^{-i\varphi_{CEP}}$ [or $\epsilon(\omega_{nn'}) = -|\epsilon(\omega_{nn'})|e^{i\varphi_{CEP}}$], where $|\epsilon(\omega_{nn'})| = \frac{F_0\sqrt{\pi}t_w}{2}$. Thus, the photoexcited state after the pulse is

$$|\Psi^{(1)}(t)\rangle = \begin{cases} -\frac{i}{\hbar}\sum_{n,n'}|\epsilon(\omega_{nn'})|e^{-i\varphi_{CEP}}\mu_{n',n}e^{-\frac{i}{\hbar}E_{n'}t}c_n|E_{n'}\rangle, & \text{for } \omega_{nn'} \geq 0 \text{ (absorption)} \\ -\frac{i}{\hbar}\sum_{n,n'}|\epsilon(\omega_{nn'})|e^{i\varphi_{CEP}}\mu_{n',n}e^{-\frac{i}{\hbar}E_{n'}t}c_n|E_{n'}\rangle, & \text{for } \omega_{nn'} < 0 \text{ (stimulated emission)} \end{cases}. \tag{22}$$

For the two-level model,

$$\begin{aligned} |\Psi^{(1)}(t)\rangle = &-\frac{i}{\hbar}|\epsilon(\omega_{01})|e^{-i\varphi_{CEP}}\mu_{10}e^{-\frac{i}{\hbar}E_1t}c_0|E_1\rangle \\ &-\frac{i}{\hbar}|\epsilon(\omega_{10})|e^{i\varphi_{CEP}}\mu_{01}e^{-\frac{i}{\hbar}E_0t}c_1|E_0\rangle \end{aligned} \tag{23}$$

so that the molecular state after photoexcitation is

$$\begin{aligned} |\Psi(t)\rangle &= |\Psi^{(0)}(t)\rangle + |\Psi^{(1)}(t)\rangle \\ &= (c_0 - \frac{i}{\hbar}|\epsilon(\omega_{10})|e^{i\varphi_{CEP}}\mu_{01}c_1)|E_0\rangle e^{-\frac{i}{\hbar}E_0t} \\ &\quad \times (c_1 - \frac{i}{\hbar}|\epsilon(\omega_{01})|e^{-i\varphi_{CEP}}\mu_{10}c_0)|E_1\rangle e^{-\frac{i}{\hbar}E_1t}. \end{aligned} \tag{24}$$

Note that the relative phase between the initial and excited state can be controlled by CEP as after photoexcitation matter picks up the CEP of the laser; $e^{-i\varphi_{CEP}}$ during absorption and $e^{i\varphi_{CEP}}$ during stimulated emission.

Using this setup, we are in a position to study the dependence of decoherence on CEPs for different initial states.

3. Decoherence dynamics: Initially separable state

Consider the case in which the system is prepared in an initially separable state $|\varepsilon_g\rangle|\chi_g\rangle$, as numerically investigated in Sec. IV A. Expanding this initial separable state in the eigenstates basis as in Eq. (17) and employing the results of first order time dependent perturbation theory in Eq. (24), the total state after photoexcitation is

$$\begin{aligned} |\Psi(t)\rangle = &(\cos(\alpha) - i\sin(\alpha)\Omega e^{i\varphi_{CEP}})e^{-\frac{i}{\hbar}E_0t}|E_0\rangle \\ &+ (-\sin(\alpha) + i\cos(\alpha)\Omega e^{-i\varphi_{CEP}})e^{-\frac{i}{\hbar}E_1t}|E_1\rangle. \end{aligned} \tag{25}$$

Here, the parameter Ω is defined as $\Omega = -\frac{|\epsilon(\omega_{01})|\mu_{10}}{\hbar}$ and $|\epsilon(\omega_{01})| = |\epsilon(\omega_{10})|$. In addition, as in the simulations, we choose $\mu_{01} = \mu_{10}$.

To calculate the purity of state Eq. (25), it is convenient to express the total state $|\Psi(t)\rangle$ in the basis $\{|g\rangle|\chi_g\rangle, |e\rangle|\chi_e\rangle\}$ as this facilitates taking the trace over the nuclei. In the notation of Eq. (18), in this case,

$$\begin{aligned} a(t) &= e^{-\frac{i}{\hbar}E_0t}(A_1 + A_2e^{-i\omega_{01}t}), \\ b(t) &= e^{-\frac{i}{\hbar}E_0t}(B_1 + B_2e^{-i\omega_{01}t}), \end{aligned} \tag{26}$$

with

$$\begin{aligned} A_1 &= \cos^2(\alpha) - i\frac{\sin(2\alpha)}{2}\Omega e^{i\varphi_{CEP}}, \\ A_2 &= \sin^2(\alpha) - i\frac{\sin(2\alpha)}{2}\Omega e^{-i\varphi_{CEP}}, \\ B_1 &= \frac{\sin(2\alpha)}{2} - i\sin^2(\alpha)\Omega e^{i\varphi_{CEP}}, \\ B_2 &= i\cos^2(\alpha)\Omega e^{-i\varphi_{CEP}} - \frac{\sin(2\alpha)}{2}. \end{aligned} \tag{27}$$

We are interested in systematic changes in the purity that survive time-averaging. We thus focus on

$$\overline{\mathcal{P}} = \lim_{t\to\infty}\frac{\int_{t_e}^{t}\mathcal{P}(t')dt'}{t - t_e} = \overline{|a(t)|^4} + \overline{|b(t)|^4} + \overline{2|a(t)|^2|b(t)|^2}S^2 \tag{28}$$

for t after photoexcitation, where the overbar denotes time-averaging and t_e is an arbitrary time after the laser pulse.

Proceeding in this way, we find that

$$\begin{aligned} \overline{|a(t)|^4} &= |A_1|^4 + |A_2|^4 + 4|A_1|^2|A_2|^2, \\ \overline{|b(t)|^4} &= |B_1|^4 + |B_2|^4 + 4|B_1|^2|B_2|^2, \\ \overline{|a(t)|^2|b(t)|^2} &= (|A_1|^2 + |A_2|^2)(|B_1|^2 + |B_2|^2) \\ &\quad + (A_1A_2^*B_1^*B_2 + A_1^*A_2B_1B_2^*). \end{aligned} \tag{29}$$

Substituting Eq. (29) into Eq. (28) yields

$$\overline{\mathcal{P}} = \mathcal{P}_0 + \left[\kappa_0(\alpha)\Omega(1-\Omega^2)\sin\varphi_{\rm CEP} + \kappa_1(\alpha)\Omega^2\sin^2\varphi_{\rm CEP}\right](1-S^2), \tag{30}$$

where

$$\kappa_0(\alpha) = \left(2\cos^6(\alpha) - 2\sin^6(\alpha) - \frac{5}{2}\sin^2(2\alpha)\cos(2\alpha)\right)\sin(2\alpha),$$
$$\kappa_1(\alpha) = \left(2\cos^4(\alpha) + 2\sin^4(\alpha) - 2\sin^2(2\alpha)\right)\sin^2(2\alpha). \tag{31}$$

Here, $\mathcal{P}_0$ is a term independent of $\varphi_{\rm CEP}$. This equation reveals that the electronic decoherence depends on CEPs, and this dependence varies with $\sin\varphi_{\rm CEP}$ and $\sin^2\varphi_{\rm CEP}$, in agreement with Eq. (5). The above equation can be further simplified by substituting $\sin(2\alpha) = -\Lambda/\sqrt{\Delta^2+\Lambda^2}$ and $\cos(2\alpha) = \Delta/\sqrt{\Delta^2+\Lambda^2}$ to yield

$$\overline{\mathcal{P}} = \mathcal{P}_0 + \frac{(2\Delta^2-\Lambda^2)\Lambda\Omega(1-S^2)}{(\Delta^2+\Lambda^2)^2(1+\Omega^2)^2} \times \left[\Delta(\Omega^2-1)\sin\varphi_{\rm CEP} + \Lambda\Omega\sin^2\varphi_{\rm CEP}\right], \tag{32}$$

where the factor $1/(1+\Omega^2)^2$ takes into account the normalization of the state to first order in perturbation theory. To test the validity of this equation, we contrasted the predictions of Eq. (32) with numerically exact computations showing identical behavior (see Fig. 7).

In the following, we discuss several physical limits and features of Eq. (32).

a. The coherent advantage. A basic question here is if there is any advantage in using coherent lasers with well-defined phases to control decoherence. To address this question, we contrast Eq. (32) with the average result expected when the laser phase is uncontrollable between realizations $\overline{\mathcal{P}}_{\rm in} = \frac{1}{2\pi}\int_0^{2\pi} d\varphi_{\rm CEP}\overline{\mathcal{P}}(\varphi_{\rm CEP})$,

$$\overline{\mathcal{P}} - \overline{\mathcal{P}}_{\rm in} = \frac{(2\Delta^2-\Lambda^2)\Lambda\Omega(1-S^2)}{(\Delta^2+\Lambda^2)^2(1+\Omega^2)^2} \times \left[\Delta(\Omega^2-1)\sin\varphi_{\rm CEP} - \frac{\Lambda\Omega}{2}\cos(2\varphi_{\rm CEP})\right]. \tag{33}$$

Since this quantity can be positive or negative depending on laser phases, thus, the laser control can mitigate or enhance the decoherence with respect to the case in which the laser phases are uncontrollable (see Fig. 7).

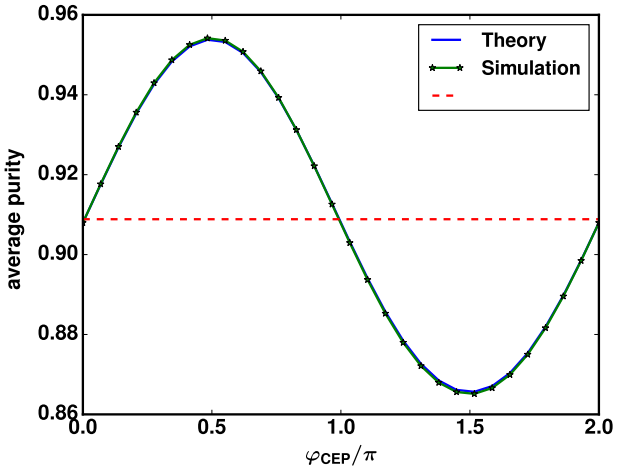

FIG. 7. Laser control map of the minimal vibronic model. The plot compares the control map (time-averaged purity vs $\varphi_{\rm CEP}$) predicted by Eq. (32) against the numerical results obtained by solving the time-dependent Schrödinger equation, showing excellent agreement. The dotted line indicates the average purity expected when the laser phase is uncontrollable. Simulations were performed by propagating the two-level vibronic system in Eq. (15) with $E_g = 0$ eV, $E_e = 2.48$ eV, and $\Lambda = 0.19$ eV. The laser parameters employed were $\hbar\omega = E_1 - E_0$, $t_w = 2$ fs, $|F_0\mu_{ge}| = 0.09$ eV, and $t_c = 20\pi/\omega$. The $\mathcal{P}_0$ value for the theory was taken from the numerical simulation for $\varphi_{\rm CEP} = 0$ as $\overline{\mathcal{P}} = \mathcal{P}_0$ in this case.

b. Diabatic couplings. For null diabatic couplings ($\Lambda = 0$), the laser control of purity disappears. In agreement with Eq. (5), the laser control only emerges when electronic transitions due to diabatic couplings play a role. However, beyond Eq. (5), these diabatic couplings Λ do not need to be spatially dependent, in agreement with the results in Fig. 4.

c. Energy gap dependence of the control. Given a fixed diabatic coupling constant Λ, the larger the energy gap Δ the smaller the range of control. The reason for this is that the larger the energy gap the closer the initial separable state becomes to the ground vibronic eigenstate for which there is no control.

d. Nuclear overlaps S. The range of control is maximum when there is zero overlap between nuclear wavepackets ($S = 0$). By contrast, for $S = 1$, the laser control disappears as there is no decoherence in this case.

e. Dominant phase dependence of the control. The control depends on $\varphi_{\rm CEP}$ as $\sin\varphi_{\rm CEP}$ and $\sin^2\varphi_{\rm CEP}$. To determine which phase dependence dominates, consider the ratio of the coefficients in front of them, $r\left(\frac{\sin\varphi_{\rm CEP}}{\sin^2\varphi_{\rm CEP}}\right) = \frac{\Delta}{\Lambda}\left(\Omega - \frac{1}{\Omega}\right)$. With $|\Omega| \gg 1$ and $|\Omega| \ll 1$, the dominant phase dependence is $\sin\varphi_{\rm CEP}$. However, with $|\Omega| \approx 1$, both $\sin\varphi_{\rm CEP}$ and $\sin^2\varphi_{\rm CEP}$ play a role in determining the decoherence timescale. In the specific case in which $|\Omega| = 1$, the control only depends on $\sin^2\varphi_{\rm CEP}$.

f. Central time of laser pulse t_c. We note that the above analysis is based on $t_c = m2\pi/\omega_{nn'}$ with positive integers m such that $t_c - 2t_w > 0$. For $t_c \neq m2\pi/\omega_{nn'}$, there is an extra phase term that depends on t_c in the calculation of the integral in Eq. (21). In fact, with different $t_c \neq m2\pi/\omega_{nn'}$, the laser control of electronic decoherence $\mathcal{P}(\varphi_{\rm CEP})$ is shifted because the phase that is picked up by the molecule during photoexcitation can be modulated by t_c. Nevertheless, the range of control of $\mathcal{P}$ remains unaffected. To exemplify this, Fig. S7 shows simulations with different central time t_c for Model I ($\lambda_0 = 0, \lambda_1 \neq 0$). As shown, the control map $\mathcal{P}(\varphi_{\rm CEP})$ is rigidly shifted by changing t_c, but the range of control remains unaffected.

4. Decoherence dynamics: Initial stationary state

We now focus on the dependence of decoherence on the CEPs when the system is initially prepared in a vibronic eigenstate, i.e., a stationary state of $H_{\rm M}$. Choosing the ground eigenstate $|E_0\rangle$ as the

initial state, the state of the system after photoexcitation is obtained from Eq. (24) by setting $c_1 = 0$ and $c_0 = 1$,

$$|\Psi(t)\rangle = e^{-\frac{i}{\hbar}E_0 t}|E_0\rangle + i\Omega e^{-\frac{i}{\hbar}E_1 t}e^{-i\varphi_{\rm CEP}}|E_1\rangle. \tag{34}$$

In this case,

$$\begin{aligned} A_1 &= \cos(\alpha), \\ A_2 &= -i\sin(\alpha)\Omega e^{-i\varphi_{\rm CEP}}, \\ B_1 &= \sin(\alpha), \\ B_2 &= i\cos(\alpha)\Omega e^{-i\varphi_{\rm CEP}}, \end{aligned} \tag{35}$$

where we have substituted Eq. (16) and used the notation in Eq. (26). The average purity can be calculated by substituting Eq. (35) into Eqs. (28) and (29). Note that in this case, because there is no initial population on the $|E_1\rangle$, all the coefficients A_1, A_2, B_1, and B_2 only include one term as Eq. (35) shows. Because of this, the CEP dependence gets canceled when calculating purity. That is, all the terms in Eq. (29) become independent of the CEP, and the laser control of decoherence dies as observed in Sec. IV B.

D. Discussion

1. Summary of observations

To summarize, we have observed laser control of electronic decoherence when the system is initially prepared in a separable electron–nuclear state and has non-zero diabatic couplings. This is consistent with the theory of electronic decoherence timescales and the perturbative analysis in Sec. IV C, which shows that few-cycle laser pulses with definitive CEP can be used to create superpositions of the form in Eq. (1) with the relative phase that can be manipulated through the CEP. Beyond the theory of electronic decoherence timescales, we have observed that the effect can survive even in cases where the diabatic couplings have no space dependence. A discussion of the origin of this effect is included in Sec. IV D 2.

While these results suggest that the laser control of electronic decoherence is possible, a more detailed investigation reveals that such laser control essentially disappears when the system is prepared in a stationary state. Thus, the observed laser control is an artifice of the assumed initially separable state. This artifice arises even in cases where such a state is an excellent approximation to the true ground state.

Below, we introduce a qualitative picture of the control that clarifies all these observations. As discussed, the non-stationary character of the initially factorizable state opens interference channels at the one-photon limit that lead to spurious laser control. We then use these insights to develop a laser control scheme of electronic decoherence that survives for arbitrary initial states.

2. Qualitative origin of the control

To develop a basic qualitative picture of the observations, it is useful to take advantage of the theoretical analysis in Sec. IV C and view the control in the molecular eigenstate basis $|E_0\rangle$, $|E_1\rangle$. When the system is prepared in an initial stationary state, the laser pulse induces a transition of the form

$$|E_0\rangle \to b_0 e^{-\frac{i}{\hbar}E_0 t}|E_0\rangle + b_1 e^{-i\varphi_{\rm CEP}}e^{-\frac{i}{\hbar}E_1 t}|E_1\rangle; \tag{36}$$

see Fig. 8(a). During resonant photoexcitation, the system picks a phase $e^{-i\varphi_{\rm CEP}}$ from the laser. However, the population of the eigenstates $|b_0|^2$ and $|b_1|^2$ is independent of the CEP. In other words, no one-photon control of the eigenstate population is possible.[31]

By contrast, when starting from a separable electron–nuclear state, one begins in a superposition of eigenstates $|\Psi(0)\rangle = c_0|E_0\rangle + d_0|E_1\rangle$. Upon photoexcitation, both absorption and stimulated emission events occur. As a consequence, the laser pulse induces a transition of the form

$$\begin{aligned} c_0|E_0\rangle + d_0|E_1\rangle \to (c_1 + c_2 e^{i\varphi_{\rm CEP}})e^{-\frac{i}{\hbar}E_0 t}|E_0\rangle \\ + (d_1 + d_2 e^{-i\varphi_{\rm CEP}})e^{-\frac{i}{\hbar}E_1 t}|E_1\rangle, \end{aligned}$$

where we have taken into account that a phase $e^{-i\varphi_{\rm CEP}}$ ($e^{i\varphi_{\rm CEP}}$) is picked up during absorption (emission), see Fig 8(b). In this case, the population of the eigenstates can be manipulated by simply varying the laser's CEP as $|c_1 + c_2 e^{i\varphi_{\rm CEP}}|^2$ and $|d_1 + d_2 e^{-i\varphi_{\rm CEP}}|^2$ depend on the CEP.

This laser phase control of the eigenstate populations for separable states ultimately leads to the control of the average purity at the subsystem level. To understand this, it is useful to note that for a general state after photoexcitation

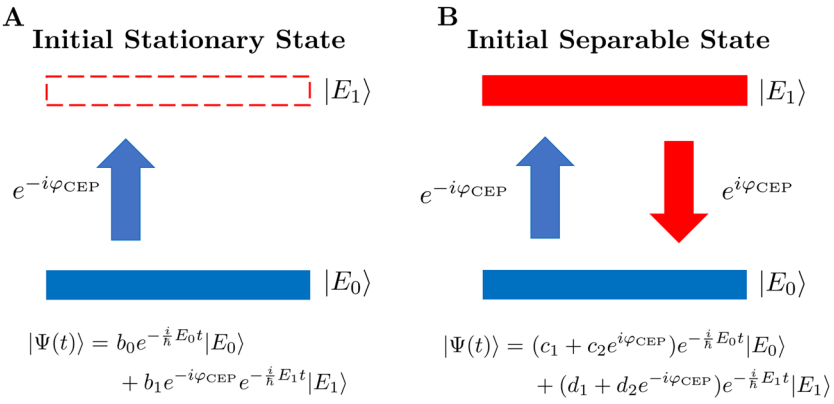

FIG. 8. Qualitative origin of the laser control of decoherence. The average purity depends on the populations of eigenstates. (a) When the system is prepared in an initial stationary state, there is no dependence of the eigenstates populations on CEP after the photoexcitation. Thus, no laser control of electronic decoherence is possible. (b) However, for initially separable states, the system is prepared in a superposition of eigenstates. This makes the eigenstates populations dependent on CEP after the photoexcitation, thus opening routes for the laser control of electronic decoherence.

$$|\Psi(t)\rangle = a_0 e^{-\frac{i}{\hbar}E_0 t}|E_0\rangle + a_1 e^{-\frac{i}{\hbar}E_1 t}|E_1\rangle, \tag{37}$$

the eigenstate populations $|a_0|^2$ and $|a_1|^2$ are related to the coefficients A_1, A_2, B_1, and B_2 that determine the average purity as in Eqs. (28) and (29) in the following form:

$$\begin{aligned} A_1 &= a_0 \cos(\alpha), \\ A_2 &= -a_1 \sin(\alpha), \\ B_1 &= a_0 \sin(\alpha), \\ B_2 &= a_1 \cos(\alpha), \end{aligned} \tag{38}$$

where we have used Eq. (26). Substituting Eq. (38) into Eq. (29), it is found that the eigenstate populations determine the dependence of average purity on the CEP. Therefore, the laser phase control of the eigenstate populations for separable states leads to control of purity and thus of the electronic decoherence.

Summarizing, the basic requirement for the CEP control of electronic decoherence is that the molecule is initially in a superposition of eigenstates that are resonantly connected by using the laser (Fig. 8). For vibronic models, this can occur when the system is initially in a separable electron–nuclear state, and the diabatic couplings V_{eg} are non-zero. If $V_{eg} = 0$, the separable initial state becomes a molecular eigenstate and the situation reduces to that schematically depicted in Fig. 8(a).

3. Is this no one-photon coherent control?

At first glance, the lack of laser control at the one-photon limit appears to be a particular case of the no one-photon coherent control theorem.[30,31] Such theorem states that the coherent control of eigenstate populations—and any other observable that commutes with the Hamiltonian—is impossible to first order in perturbation theory when the system is initially prepared in a stationary state. Even for observables that do not commute with the Hamiltonian, the theorem applies when one is interested in time-averaged quantities and the observable has no intrinsic time-dependence[31] (i.e., when the operator $\hat{O}$ in the Schrödinger picture has no time-dependence). In the minimal model, the calculation reveals that the purity depends on the eigenstate populations, and therefore, if such populations are not controllable, the purity is also not controllable. Thus, the time-averaged purity for the minimal model clearly satisfies the no one-photon coherent control theorem. In addition, the numerical results in two generic models show that the control essentially disappears when the system is prepared in an eigenstate.

However, at least formally, the electronic purity should be controllable at the one-photon limit. This is because the electronic density matrix $\sigma(t)$, which is the observable associated with electronic purity, does not commute with the Hamiltonian and has an intrinsic time dependence. Subsystem purity is thus beyond the scope of the one-photon theorem of coherent control. In fact, the numerical computations show that the laser control is technically non-zero, albeit small (see insets in Fig. 5).

V. TWO-PULSE COHERENT CONTROL OF ELECTRONIC DECOHERENCE

From the analysis above, it becomes clear that to exert active control of electronic decoherence through laser phases starting from an eigenstate, one can propose the following two-pulse scenario: (1) First, a few-cycle laser pulse with fixed CEP (i.e. $\varphi_{\mathrm{CEP}}^{(1)} = 0$) is used to resonantly photoexcite the system and create a superposition state of the form

$$|\Psi(t)\rangle = c_0|E_0\rangle + d_0|E_1\rangle. \tag{39}$$

(2) Subsequently, a second few-cycle laser pulse resonant with the same two levels with varying CEP $\varphi_{\mathrm{CEP}}^{(2)}$ can be employed to generate interference in the eigenstate populations and thus the control of the electronic decoherence.

To demonstrate this, Figs. 9 and 10 show the decoherence dynamics starting from the ground nuclear eigenstate under

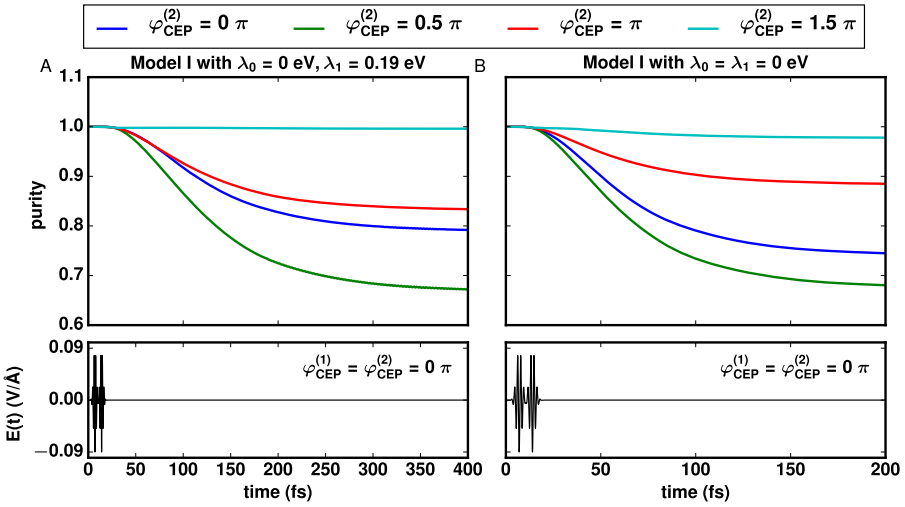

FIG. 9. Two-pulse laser control of electronic decoherence in Model I starting from the ground stationary state. The plot shows the purity dynamics during and after photoexcitation with two few-cycle laser pulses. The CEP of the first pulse is fixed at $\varphi_{\mathrm{CEP}}^{(1)} = 0$, while that of the second one $\varphi_{\mathrm{CEP}}^{(2)}$ is varied. The top panels contrast the purity dynamics with (a) non-zero ($\lambda_0 = 0$ eV, $\lambda_1 = 0.19$ eV) and (b) zero ($\lambda_0 = \lambda_1 = 0$ eV) diabatic couplings. The bottom panels show the train of laser pulses employed for $\varphi_{\mathrm{CEP}}^{(1)} = \varphi_{\mathrm{CEP}}^{(2)} = 0$.

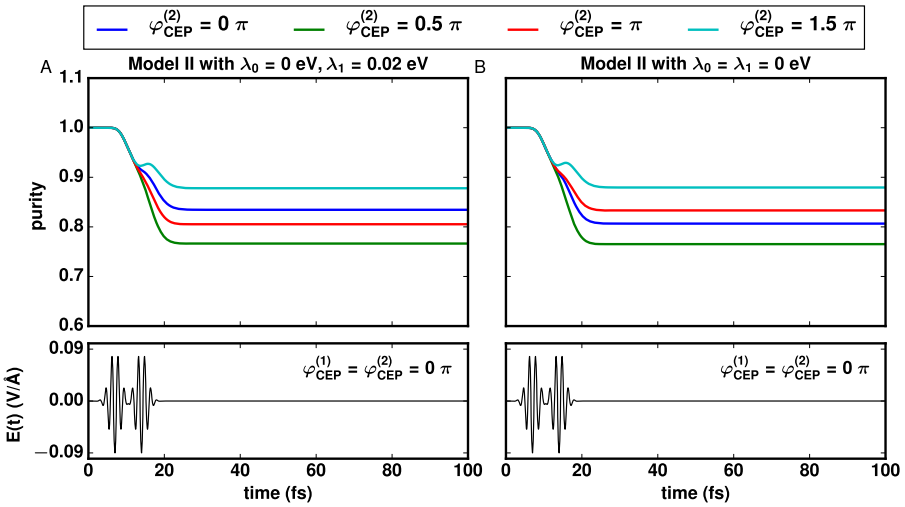

FIG. 10. [(a) and (b)] Two-pulse laser control of electronic decoherence in Model II starting from the ground stationary state. The organization of the plot is identical to that in Fig. 9.

the influence of this two-pulse control scheme with varying $\varphi^{(2)}_{CEP}$ of the second pulse. Figure 9 details the dynamics of Model I, while Fig. 10 focuses on Model II. For both models, the width of employed laser pulses is $t^{(n)}_w = 2$ fs (n = 1, 2) and the pulse center of the first laser is $t^{(1)}_c = 7$ fs, while $t^{(2)}_c = 14$ fs. As shown, the purity dynamics can be strongly manipulated by varying $\varphi^{(2)}_{CEP}$ in both cases. This type of control emerges even without diabatic couplings [see Figs. 9(b) and 10(b)]. The reason why the diabatic couplings are not needed is that the first laser pulse creates the superposition of eigenstates required for the emergence of the control. This two-laser pulse control scenario is reminiscent to pump–probe and bichromatic control strategies.[2]

To understand if this laser control arises due to the control of the populations (σ_{00}, σ_{11}) or the coherence (σ_{01}) in the electronic density matrix expressed in the basis of diabatic states, we decomposed the purity dynamics $\mathcal{P} = \sigma^2_{00} + \sigma^2_{11} + 2|\sigma_{01}|^2$ into these two contributions. Figures 11 and 12 show this decomposition for Model I and II, respectively. As shown, the laser control scenario manipulates both the populations and the coherences. After the laser, the coherences decay and the asymptotic purity is due to the populations of the diabatic states.

The next question that arises is the extent to which the two laser pulses can be separated in time while still maintaining the laser phase control. To test this, we performed simulations with pulses separated by increasingly longer times Δt. In Model I (Fig. 13), we observe that the effect survives for pulses separated by Δt = 0 fs, 4 fs, 143 fs, and even 223 fs! By contrast, in Model II (Fig. 14), we observe that the control is lost when the pulses are separated even by just 13 fs. We observe that to generate control, the two pulses need to interact with the system before the coherences in the diabatic basis induced by the first pulse disappear. While for Model I, such coherence

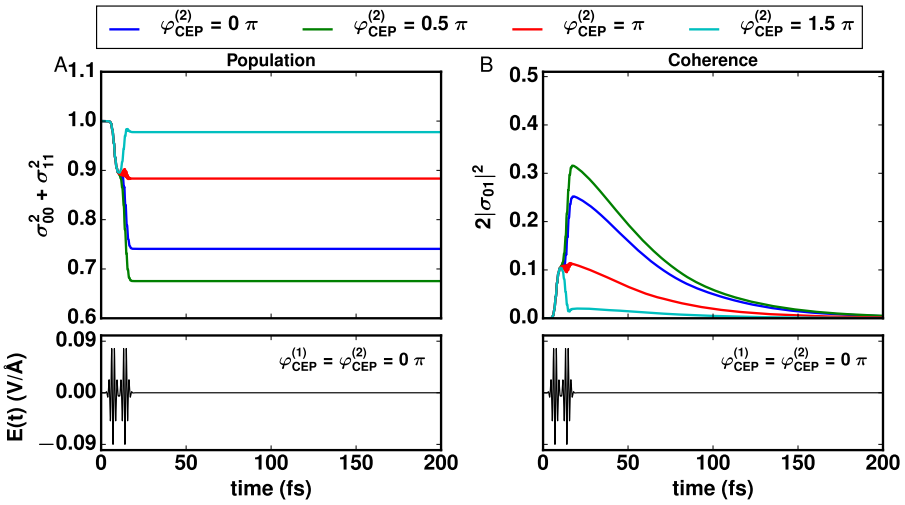

FIG. 11. Model I. (a) Population (σ^2_{00} + σ^2_{11}) and (b) coherence ($2|\sigma_{01}|$) contributions to the purity dynamics in the two-pulse laser control of electronic decoherence (λ_0 = λ_1 = 0 eV). Modeling conditions are identical to those in Fig. 9(b).

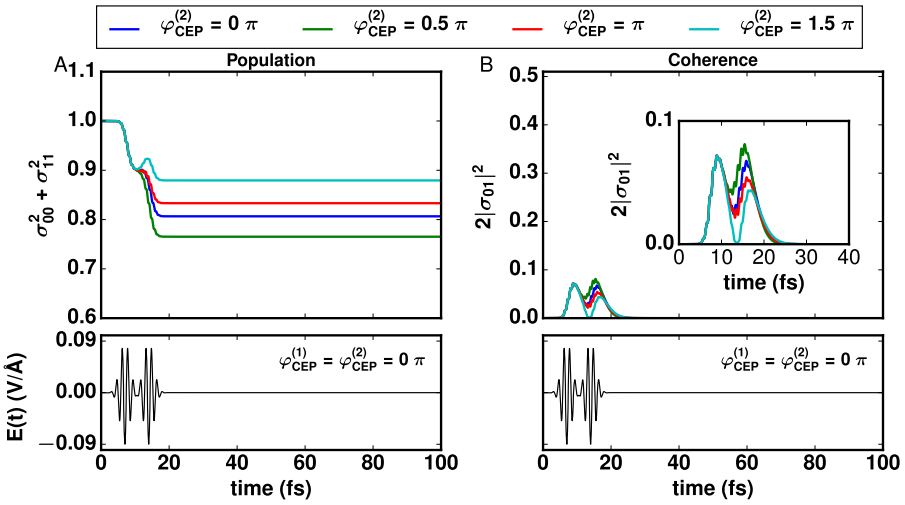

FIG. 12. Model II. (a) Population ($\sigma^2_{00} + \sigma^2_{11}$) and (b) coherence ($2|\sigma_{01}|$) contributions to the purity dynamics in the two-pulse laser control of electronic decoherence ($\lambda_0 = \lambda_1 = 0$ eV). Modeling conditions are identical to those in Fig. 10(b).

persists for ~200 fs [see Fig. 11(b)], in Model II, they decay in ~20 fs [see Fig. 12(b)]. Such coherences are essential for the emergence of the effect.

In the single pulse schemes in Sec. IV, the control map is shifted by changing the turn-on time of the laser pulse (see Sec. IV C and Fig. S7). By contrast, here, the control depends on relative quantities that are simpler to manipulate: the phase difference $\varphi^{(1)}_{CEP} - \varphi^{(2)}_{CEP}$ and the time delay between pulses $t^{(1)}_c - t^{(2)}_c$. This result follows by considering the two-pulse photoexcitation using second order perturbation theory.

While this route to control was exemplified in low-dimensional models, the basic strategy is expected to work in higher dimensional systems too. This is because the low-dimensional models contain all the decoherence channels for a generic molecule[43,44] and the control does not rely in recurrences in wavepacket motion that are not typically observed in systems of higher dimensionality.[35]

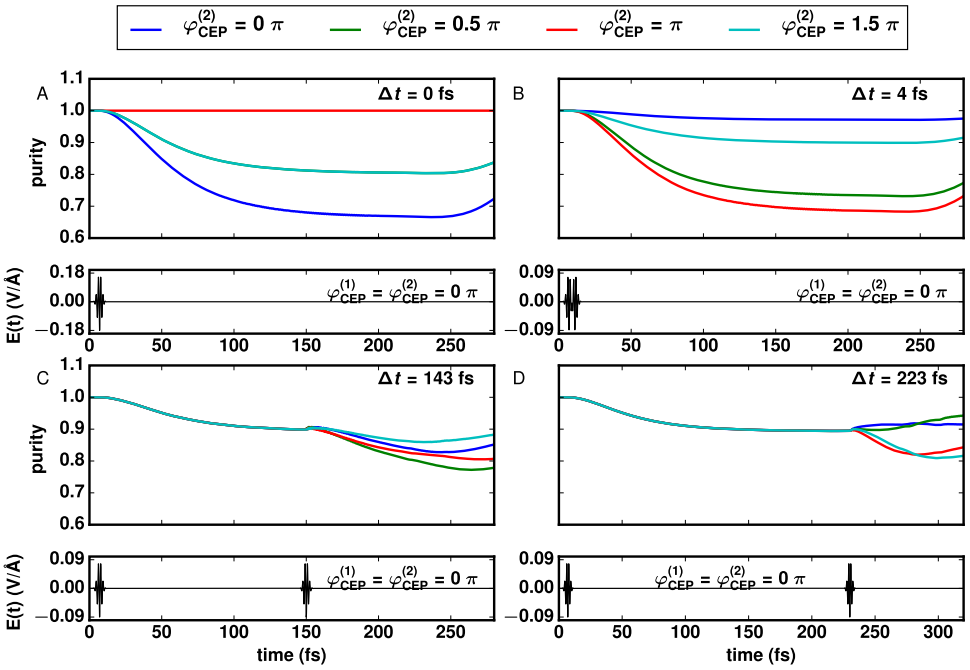

FIG. 13. Two-pulse laser control of electronic decoherence for varying laser-pulse time separation Δt in Model I ($\lambda_0 = 0$ eV, $\lambda_1 = 0.19$ eV) starting from the ground stationary state. The plot shows the purity dynamics and the corresponding laser pulses with Δt (a) 0 fs, (b) 4 fs, (c) 143 fs, and (d) 223 fs. Note that the laser control persists even with $\Delta t = 223$ fs.

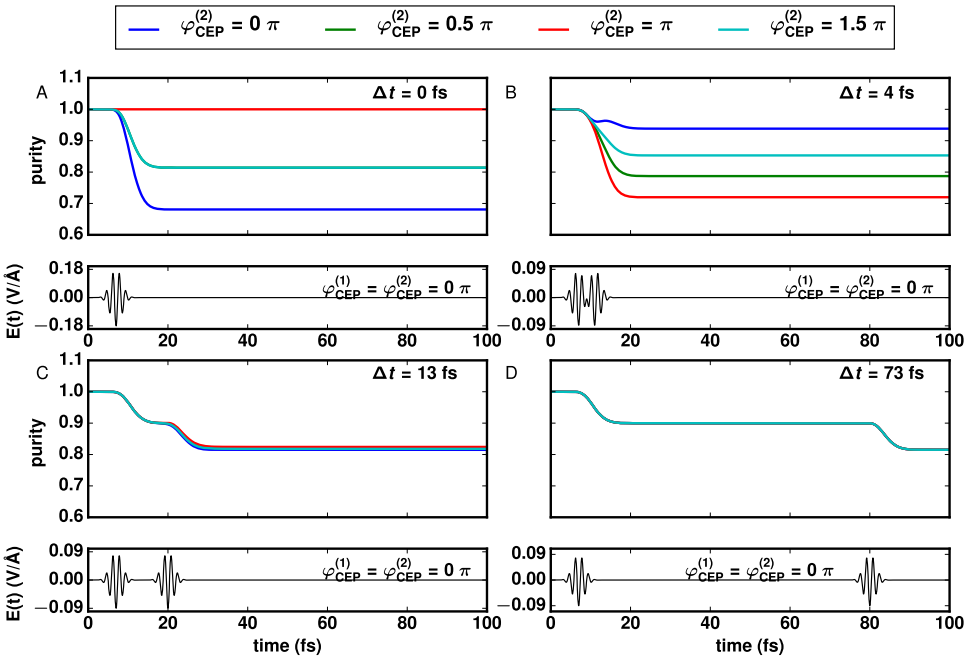

FIG. 14. Two-pulse laser control of electronic decoherence for varying laser-pulse time separation Δt in Model II ($\lambda_0 = 0$ eV, $\lambda_1 = 0.02$ eV) starting from the ground stationary state. The plot shows the purity dynamics and the corresponding laser pulses with Δt (a) 0 fs, (b) 4 fs, (c) 13 fs, and (d) 73 fs. Note that the laser control disappears when the Δt is beyond 13 fs.

VI. CONCLUSION

In this work, we investigated the possibility to achieve laser control of electronic decoherence using ultrafast few-cycle laser pulses with well-defined carrier envelope phase (CEP). This possibility was opened by recent advances in the theory[26,27] and simulations[28] of electronic decoherence, which indicates that it is possible to manipulate the rate of electronic coherence loss via the control of the relative phase in the initial electronic superposition state. However, the actual laser implementation of such a concept is an open challenge. By computing the purity dynamics in two exemplifying molecular models (photoisomerization and displaced harmonic oscillator) through actual laser photoexcitation, we found that such initial superposition state and the subsequent laser control of electronic decoherence can be created using a few-cycle laser pulse with various CEPs in the weak-field limit, provided that the system is initially prepared in a separable electron–nuclear state. This one-photon laser control, however, disappears when the molecule is initially prepared in a stationary molecular state. Through a detailed analysis of the origins of these intriguing observations, we found that the non-stationary character of the initial separable state is essential for the laser control. That is, the one-photon laser control of electronic decoherence is an artifice introduced by the often-used initial separable state. This artifice emerges even when the initially separable state is an excellent approximation to the eigenstate of the composite system with fidelities above 98.5%. The fact that we observe similar behavior in two different exemplifying models highlights the generality of the observations.

To better understand these observations, we introduced a minimal theoretical model that showed that the reason why initial separable states open one-photon control pathways is because these states are superpositions of stationary molecular states. Such a superposition opens interference channels even at the single-photon limit that can be manipulated through laser phases.

Based on this theoretical analysis, we designed a two-pulse control scheme that enables the laser control of electronic decoherence even when the molecule is initially prepared in a stationary molecular state. In this scheme, the first pulse is used to create a vibronic superposition state and the second one to generate phase-controllable interference. By varying the relative carrier envelope phase between the two pulses, it is possible to suppress or enhance the purity decay.

These results identify a viable scheme for the laser control of electronic decoherence and expose a surprising artifact that is introduced by often-used initially factorizable system–bath states in the field of open quantum systems. The control scenario is based on impulsive excitation with lasers with a well-defined carrier envelope phase in the weak-field limit. Future prospects include determining the utility of other strategies such as chirping[45,46] and strong field strategies for the laser control of electronic decoherence beyond the impulsive limit.

SUPPLEMENTARY MATERIAL

See the supplementary material for additional figures testing the convergence of the method and further exploring the parameter space of the identified phenomenology.

ACKNOWLEDGMENTS

This material is based on the work supported by the National Science Foundation under Grant No. CHE-1553939.

REFERENCES

[1] M. A. Nielsen and I. L. Chuang, *Quantum Computation and Quantum Information* (Cambridge University Press, 2011).
[2] M. Shapiro and P. Brumer, *Principles of the Quantum Control of Molecular Processes* (Wiley-Interscience, 2003).
[3] S. Rice and M. Zhao, *Optical Control of Molecular Dynamics* (Wiley, 2000).
[4] H. P. Breuer and F. Petruccione, *The Theory of Open Quantum Systems* (Oxford University Press, 2002).
[5] G. D. Scholes *et al.*, Nature **543**, 647 (2017).
[6] E. Meneghin *et al.*, Nat. Commun. **9**, 3160 (2018).
[7] F. Ma, E. Romero, M. R. Jones, V. I. Novoderezhkin, and R. van Grondelle, Nat. Commun. **10**, 933 (2019).
[8] J. D. Roscioli, S. Ghosh, A. M. LaFountain, H. A. Frank, and W. F. Beck, J. Phys. Chem. Lett. **9**, 5071 (2018).
[9] A. Dodin and P. Brumer, J. Chem. Phys. **150**, 184304 (2019).
[10] D. Abramavicius and S. Mukamel, J. Chem. Phys. **133**, 064510 (2010).
[11] G. Panitchayangkoon, D. V. Voronine, D. Abramavicius, J. R. Caram, N. H. C. Lewis, S. Mukamel, and G. S. Engel, Proc. Natl. Acad. Sci. U. S. A. **108**, 20908 (2011).
[12] G. S. Engel, T. R. Calhoun, E. L. Read, T.-K. Ahn, T. Mančal, Y.-C. Cheng, R. E. Blankenship, and G. R. Fleming, Nature **446**, 782 (2007).
[13] L. Wang, M. A. Allodi, and G. S. Engel, Nat. Rev. Chem. **3**, 477 (2019).
[14] N. V. Golubev and A. I. Kuleff, Phys. Rev. A **91**, 051401 (2015).
[15] F. Krausz and M. Ivanov, Rev. Mod. Phys. **81**, 163 (2009).
[16] F. Lépine, M. Y. Ivanov, and M. J. J. Vrakking, Nat. Photonics **8**, 195 (2014).
[17] M. Lara-Astiaso, D. Ayuso, I. Tavernelli, P. Decleva, A. Palacios, and F. Martín, Faraday Discuss. **194**, 41 (2016).
[18] S. Mukamel, *Principles of Nonlinear Optical Spectroscopy* (Oxford University Press, 1995).
[19] E. Joos, H. D. Zeh, C. Kiefer, D. J. Giulini, J. Kupsch, and I.-O. Stamatescu, *Decoherence and the Appearance of a Classical World in Quantum Theory* (Springer Science & Business Media, 2013).
[20] A. Rényi, in *Proceedings of the Fourth Berkeley Symposium on Mathematical Statistics and Probability* (University of California Press, 1961), Vol. 1, pp. 547–561.
[21] A. F. Izmaylov and I. Franco, J. Chem. Theory Comput. **13**, 20 (2017).
[22] A. Schiffrin, T. Paasch-Colberg, N. Karpowicz, V. Apalkov, D. Gerster, S. Mühlbrandt, M. Korbman, J. Reichert, M. Schultze, S. Holzner, J. V. Barth, R. Kienberger, R. Ernstorfer, V. S. Yakovlev, M. I. Stockman, and F. Krausz, Nature **493**, 70 (2013).
[23] L. Chen, Y. Zhang, G. Chen, and I. Franco, Nat. Commun. **9**, 2070 (2018).
[24] T. Higuchi, C. Heide, K. Ullmann, H. B. Weber, and P. Hommelhoff, Nature **550**, 224 (2017).
[25] E. Vella, H. Li, P. Grégoire, S. M. Tuladhar, M. S. Vezie, S. Few, C. M. Bazán, J. Nelson, C. Silva-Acuña, and E. R. Bittner, Sci. Rep. **6**, 29437 (2016).
[26] B. Gu and I. Franco, J. Phys. Chem. Lett. **8**, 4289 (2017).
[27] B. Gu and I. Franco, J. Phys. Chem. Lett. **9**, 773 (2018).
[28] C. Arnold, O. Vendrell, R. Welsch, and R. Santra, Phys. Rev. Lett. **120**, 123001 (2018).
[29] C. Homann, M. Bradler, M. Förster, P. Hommelhoff, and E. Riedle, Opt. Lett. **37**, 1673 (2012).
[30] P. Brumer and M. Shapiro, Chem. Phys. **139**, 221 (1989).
[31] M. Spanner, C. A. Arango, and P. Brumer, J. Chem. Phys. **133**, 151101 (2010).
[32] M. Beau, J. Kiukas, I. L. Egusquiza, and A. del Campo, Phys. Rev. Lett. **119**, 130401 (2017).
[33] O. V. Prezhdo and P. J. Rossky, Phys. Rev. Lett. **81**, 5294 (1998).
[34] L. Allen and J. Eberly, *Optical Resonance and Two-Level Atoms* (Dover, 1975).
[35] W. Hu, B. Gu, and I. Franco, J. Chem. Phys. **148**, 134304 (2018).
[36] S. Hahn and G. Stock, J. Phys. Chem. B **104**, 1146 (2000).
[37] S. Dilthey and G. Stock, Phys. Rev. Lett. **87**, 140404 (2001).
[38] G. Stock and M. Thoss, "Classical description of nonadiabatic quantum dynamics," in *Advances in Chemical Physics* (Wiley-Blackwell, 2005), Chap. 5, pp. 243–375.
[39] R. Kosloff, J. Phys. Chem. **92**, 2087 (1988).
[40] I. Franco and P. Brumer, J. Chem. Phys. **136**, 144501 (2012).
[41] C. Arnold, O. Vendrell, and R. Santra, Phys. Rev. A **95**, 033425 (2017).
[42] D. J. Tannor, *Introduction to Quantum Mechanics* (University Science Books, 2007).
[43] L. S. Cederbaum, E. Gindensperger, and I. Burghardt, Phys. Rev. Lett. **94**, 113003 (2005).
[44] I. G. Ryabinkin, L. Joubert-Doriol, and A. F. Izmaylov, J. Chem. Phys. **140**, 214116 (2014).
[45] C. A. Arango and P. Brumer, J. Chem. Phys. **138**, 071104 (2013).
[46] G. Katz, M. A. Ratner, and R. Kosloff, New J. Phys. **12**, 015003 (2010).